Equivalent Single-Span Model for Dispersion-Managed Fiber-Optic Transmission Systems

Johannes Karl Fischer, *Student Member, IEEE*, Christian-Alexander Bunge, *Member, IEEE*, and Klaus Petermann, *Fellow, IEEE*

***Abstract*—This paper reviews the application of the Volterra series expansion to fiber-optic communication systems and performance evaluation of dispersion maps. It is shown that under certain conditions periodically dispersion-managed multispan systems can be approximated by simple single-span systems with dispersion precompensation. This single-span approximation can help us to identify equivalent system configurations and estimate optimum system parameters. To set an example, the single-span model is employed to analyze transmission systems based on the return-to-zero on–off-keying modulation format and direct detection.**

***Index Terms*—Dispersion management, fiber nonlinearity, Volterra series expansion.**

I. Introduction

THE capacity and reach of fiber-optic communication systems are limited by the inherent nonlinearity of the transmission medium silica fiber. A very effective approach to minimize accumulation of nonlinear distortion along fiber-optic links is the optimization of the cumulated dispersion profile, commonly referred to as dispersion management. Based on the Volterra series expansion, we propose a single-span model of fiber-optic links, which can be used to simplify this time-consuming optimization process.

The Volterra series expansion as a tool to model nonlinear systems has been applied to optical fibers by Peddanarappagari and Brandt-Pearce in 1997 [1]. Since then it has been successfully used to model interchannel nonlinear effects such as cross-phase modulation (XPM) and four-wave mixing (FWM), which can be major impairments in fiber-optic wavelength-division multiplexing (WDM) transmission systems [2]. More recently, a time-domain counterpart of the frequency-domain Volterra transfer function—the power-weighted dispersion distribution function—was applied to analytically derive the generation of ghost pulses due to intrachannel four-wave mixing (IFWM) in high-speed pulse-overlapped transmission [3]. The major drawback of the Volterra series expansion is its slow convergence and insufficient accuracy for large input powers, i.e., in the highly nonlinear regime. Although its accuracy is comparable to other alternative methods such as the regular perturbation approach [4], it should only be applied under the condition of a weakly nonlinear regime [5].

Manuscript received March 28, 2008; revised July 17, 2008 and August 27, 2008. First published May 02, 2009; current version published July 29, 2009.

The authors are with the Technische Universität Berlin, Fachgebiet Hochfrequenztechnik-Photonics HFT 4, 10587 Berlin, Germany (e-mail: j.k.fischer@ieee.org; christian-alexander.bunge@tu-berlin.de; petermann@tu-berlin.de).

Digital Object Identifier 10.1109/JLT.2008.2005513

Proper dispersion management can reduce the accumulation of nonlinear distortion in fiber-optic transmission systems. Consequently, Louchet applied the Volterra series to systems with single-periodic dispersion maps and derived a closed form solution for the received optical signal. However, the described equivalent single-fiber model does not account for dispersion precompensation [6]. In the present paper, we extend this approach to a more general class of systems, including dispersion precompensation and randomly varying residual dispersion per span. Furthermore, we propose an approximation of the third-order Volterra kernel transform in order to yield an equivalent single-span description with simple parameters to characterize the nonlinear properties of a wide range of possible system configurations. This single-span approximation is in line with important design rules derived in recent years, pertaining to the dependence of nonlinear impairments on cumulated nonlinear phase [7], bit rate, and fiber dispersion [8], [9] and dispersion map [10], [11]. It is shown that these design rules define the parameters of the equivalent single-span system and thus the approximate first-order nonlinear perturbation.

This paper is organized as follows. In Section II, we start by introducing the nonlinear transfer function of a single fiber and subsequently include dispersion precompensation and residual dispersion per span in a system consisting of multiple fiber spans. Finally, a randomly varying residual dispersion as it is common in practical systems is also considered. Section III presents a possible application of the model by an exemplary analysis of systems based on the return-to-zero on–off-keying (RZ-OOK) modulation format.

II. The Nonlinear Transfer Function

Propagation of the complex envelope $A(T,z)$ of the electric field along the spatial coordinate z of a single-mode fiber is described by the well-known nonlinear Schrödinger equation. Neglecting higher order dispersion and stimulated inelastic scattering processes, such as stimulated Raman scattering, it can be expressed in the time domain as [12]

$$\frac{\partial A(T,z)}{\partial z} = -\frac{\alpha}{2}A(T,z) - j\frac{\beta_2}{2}\frac{\partial^2 A(T,z)}{\partial T^2} + j\gamma\left|A(T,z)\right|^2 A(T,z) \quad (1)$$

where $T = t - \beta_1 z$ is a retarded time frame moving with the group velocity $v_{\mathrm{gr}} = 1/\beta_1$, β_2 is the group-velocity dispersion, α is the attenuation coefficient of the fiber, and γ is its nonlinear

coefficient. In order to derive the frequency-domain Volterra series, it is practical to transform (1) into the frequency domain. The Fourier transform of (1) is

$$\frac{\partial \tilde{A}(\omega,z)}{\partial z} = -\frac{\alpha}{2}\tilde{A}(\omega,z) + j\omega^2\frac{\beta_2}{2}\tilde{A}(\omega,z) + j\gamma\int\int \tilde{A}(\omega_1,z)\tilde{A}^*(\omega_2,z)\tilde{A}(\omega_3,z)d\omega_1 d\omega_2 \quad (2)$$

where $\tilde{A}(\omega,z)$ is the Fourier transform of $A(T,z)$ and $\omega_3 = \omega - \omega_1 + \omega_2$ for brevity. In a weakly nonlinear regime, the complex envelope $\tilde{A}(\omega,z)$ can be approximated with the Volterra series expansion up to third order as [1]

$$\tilde{A}(\omega,z) \approx H_1(\omega,z)\tilde{A}_0(\omega) + \int\int H_3(\omega_1,\omega_2,\omega,z) \times \tilde{A}_0(\omega_1)\tilde{A}_0^*(\omega_2)\tilde{A}_0(\omega_3)d\omega_1 d\omega_2 \quad (3)$$

where $\tilde{A}_0(\omega)$ stands for $\tilde{A}(\omega, z = 0)$, and $H_1(\omega,z)$ and $H_3(\omega_1,\omega_2,\omega,z)$ are the first- and third-order Volterra kernel transforms, respectively. In the following, we note $\tilde{S}_0 = \tilde{A}_0(\omega_1)\tilde{A}_0^*(\omega_2)\tilde{A}_0(\omega_3)$ for conciseness of notation. The kernel transforms are determined by substituting (3) into (2). After some calculations (for convenience a detailed derivation is given in Appendixes I and II), the complex envelope of the electric field after transmission over M fiber sections can be approximated in the frequency domain as

$$\tilde{A}_{\mathrm{M}}(\omega) \approx H_1(\omega)\left(\tilde{A}_0(\omega) + \delta_{\mathrm{NL}}(\omega)\right) \quad (4)$$

where $\delta_{\mathrm{NL}}(\omega)$ is a small perturbation of the linear solution due to fiber nonlinearity. The nonlinear perturbation can be expressed through a double convolution as [6]

$$\delta_{\mathrm{NL}}(\omega) = j\int\int \eta(\Delta\Omega)\tilde{S}_0 d\omega_1 d\omega_2, \quad (5)$$

where $\Delta\Omega = (\omega-\omega_1)(\omega_1-\omega_2)$. The nonlinear transfer function $\eta(\Delta\Omega)$ depends on the physical parameters of the transmission system and is signal independent. For a concatenation of M fiber sections, the nonlinear transfer function can be written in the following form:

$$\eta(\Delta\Omega) = \sum_{m=1}^{\mathrm{M}} \gamma_m e^{G_m + j\widetilde{D}_m\Delta\Omega}\int_0^{L_m} e^{(-\alpha_m - j\beta_{2,m}\Delta\Omega)z}dz, \quad (6)$$

where G_m and $\widetilde{D}_m$ are the cumulated gain and dispersion at the beginning of the *m*th fiber, and L_m, $\beta_{2,m}$, α_m and γ_m are the length, group-velocity dispersion, attenuation, and nonlinear coefficient of the *m*th fiber, respectively. Please note that throughout this paper cumulated dispersion in units ps/nm is denoted by D_m. The relation between this parameter and $\widetilde{D}_m$ in (6) is $\widetilde{D}_m = \lambda^2 D_m/(2\pi c)$, with wavelength λ and the speed of light c. Using this notation $\widetilde{D}_m$ and D_m have the same sign, but $\widetilde{D}_m$ has units ps^2.

The key assumptions for (4)–(6) to be valid are as follows.

1) Small signal power and thus small nonlinear perturbation verifying $\int|\delta_{\mathrm{NL}}(\omega)|^2 d\omega \ll \int|\tilde{A}_0(\omega)|^2 d\omega$, i.e., operation in a weakly nonlinear transmission regime [1], [5].
2) Higher order nonlinear perturbative terms are assumed to be negligible. This condition may not be fulfilled for high-span counts.
3) Nonlinear interaction between amplifier noise and signal (e.g., Gordon–Mollenauer phase noise [13]) must be negligible. This condition may not be fulfilled for high-span counts or systems operating at a low-optical signal-to-noise ratio (OSNR) and can be problematic when dealing with phase-modulated signals.

A. Single-Span System

Assuming a single fiber with length $L \gg 1/\alpha$, the nonlinear transfer function of this fiber is obtained from (6) with $M = 1$ as

$$\eta_s(\Delta\Omega) \approx \frac{\gamma}{\alpha}\frac{1}{1 - j\frac{\Delta\Omega}{\Omega_s}} \quad (7)$$

where $\Omega_s = -\alpha/\beta_2$ is its 3 dB bandwidth which is related through $\Omega_s = 4\pi f_d^2$ to the nonlinear diffusion bandwidth derived in [6]. An analogue expression for the single-span kernel has been derived through averaged propagation models in earlier contributions by Turitsyn and coworkers [14], [15].

Relating the bandwidth Ω_s to a measure for the spectral width of the input signal, e.g., to the bit rate B as B^2/Ω_s, yields a dimensionless parameter which is a direct measure for the maximum number of overlapping and nonlinearly interacting pulses in a single-wavelength channel within the effective length $L_{\mathrm{eff}} \approx 1/\alpha$ of a fiber [16]. Therefore, it universally describes the strength of intrachannel nonlinear effects. This result was also obtained empirically by numerical simulations in [9] and without inclusion of the attenuation coefficient in [8]. Furthermore, (7) is closely related to the impact of FWM, where $\beta_2\Delta\Omega$ describes the phase mismatch of the interacting fields, and $|\eta_s|^2$ is the efficiency of the FWM process [17].

Fig. 1 shows the magnitude and phase of the transfer function as a function of $\Delta\Omega$ for 80 km of nonzero dispersion-shifted fiber (NZDSF) with a dispersion parameter of $D = 4\ \mathrm{ps}/(\mathrm{nm}\cdot\mathrm{km})$ and standard single-mode fiber (SSMF) with $D = 16\ \mathrm{ps}/(\mathrm{nm}\cdot\mathrm{km})$. Lower local dispersion leads to a broadening of the transfer function. Consequently, more frequency components of the input signal participate significantly in the nonlinear processes affecting the signal at angular frequency ω. This reflects the well-known fact that the impact of FWM is more severe at lower local dispersion [17], [18].

Commonly, a certain amount of dispersion precompensation is used to predistort the launched signal at the transmitter and thereby reduce the impact of fiber nonlinearity on the signal [19], [20]. Assuming linear transmission through the precompensating fiber, dispersion precompensation can be included in the single-fiber transfer function through the cumulated dispersion profile $\widetilde{D}(z)$. For a single fiber with precompensation, the cumulated dispersion is $\widetilde{D}(z) = -\beta_2 z + \widetilde{D}_{\mathrm{pre}}$, where $\widetilde{D}_{\mathrm{pre}}$ is the amount of dispersion precompensation in units ps^2. With (6), the transfer function of a single fiber preceded by dispersion precompensation is then

$$\eta(\Delta\Omega) \approx \eta_s(\Delta\Omega)e^{j\widetilde{D}_{\mathrm{pre}}\Delta\Omega}. \quad (8)$$

Introducing a precompensation thus only affects the phase of the nonlinear transfer function and has no effect on its magnitude.

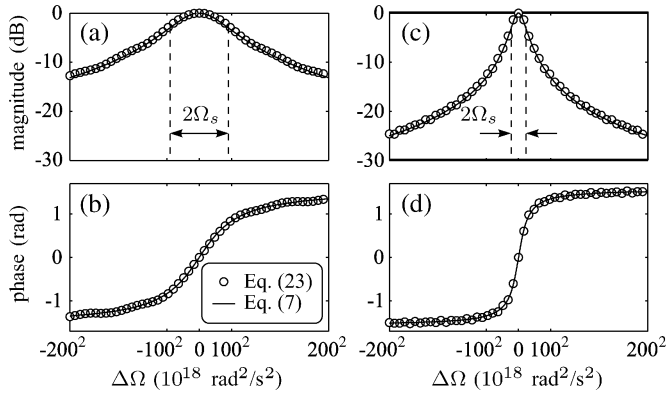

Fig. 1. Normalized magnitude and phase of the single-span nonlinear transfer function $\eta_s(\Delta\Omega)$ for $L = 80\,\mathrm{km}$, $\alpha = 0.2\,\mathrm{dB/km}$, and (a,b) $D = 4\,\mathrm{ps/(nm\cdot km)}$, i.e., $\Omega_s = 9 \cdot 10^{21}\,\mathrm{rad^2/s^2}$, and (c,d) $D = 16\,\mathrm{ps/(nm \cdot km)}$, i.e., $\Omega_s = 2.25 \cdot 10^{21}\,\mathrm{rad^2/s^2}$ at a wavelength of $\lambda = 1.55\,\mu$m. Shown are the exact function according to (23) (circles) and its approximation according to (7) (line).

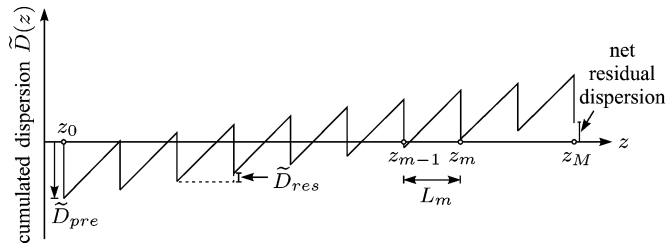

Fig. 2. Profile of the cumulated dispersion in a single-periodic dispersion map with dispersion precompensation $\widetilde{D}_{\mathrm{pre}}$ and residual dispersion per span $\widetilde{D}_{\mathrm{res}}$.

B. Single-Periodic Dispersion Maps

A common scheme for dispersion management is the single-periodic dispersion map [20]. Ideally, it consists of N identical spans, each comprising of a transmission fiber and a dispersion-compensating fiber (DCF). Depending on the length of the DCF there is usually a certain amount of residual dispersion per span. The dispersion profile $\widetilde{D}(z)$ of such a map is shown in Fig. 2. Assuming low input power into the DCF and thus negligible nonlinear impact, they act as ideal lumped dispersion compensation modules at positions z_m. Under the assumption of identical spans, the length, attenuation, group-velocity dispersion, and nonlinear coefficients of the transmission fibers are the same in each span, and (6) simplifies to [6]

$$\eta(\Delta\Omega) = \frac{\gamma}{\alpha}\frac{1 - e^{-\alpha L - j\beta_2 L\Delta\Omega}}{1 + j\frac{\beta_2}{\alpha}\Delta\Omega}\sum_{n=1}^{N} e^{G_n + j\widetilde{D}_n\Delta\Omega}. \quad (9)$$

Further simplification is possible by noting that loss is usually compensated per span (i.e., $G_n = 0$) and fibers are relatively long (i.e., $L \gg 1/\alpha$). Assuming identical spans means that there is a constant residual dispersion per span $\widetilde{D}_{\mathrm{res}}$. With the cumulated dispersion at the beginning of the nth span $\widetilde{D}_n = \widetilde{D}_{\mathrm{pre}} + (n-1)\widetilde{D}_{\mathrm{res}}$ (9) can be written as

$$\eta(\Delta\Omega) \approx \eta_s(\Delta\Omega)e^{j\widetilde{D}_{\mathrm{pre}}\Delta\Omega}\sum_{n=1}^{N} e^{j(n-1)\widetilde{D}_{\mathrm{res}}\Delta\Omega} \quad (10)$$

with the nonlinear transfer function of a single fiber η_s according to (7). Evaluating the geometric series in (10) yields

$$\begin{aligned}\eta(\Delta\Omega) &\approx \eta_s(\Delta\Omega)\frac{e^{jN\widetilde{D}_{\mathrm{res}}\Delta\Omega} - 1}{e^{j\widetilde{D}_{\mathrm{res}}\Delta\Omega} - 1}e^{j\widetilde{D}_{\mathrm{pre}}\Delta\Omega} \\ &\approx \eta_s(\Delta\Omega)\frac{\sin\left(\frac{N}{2}\widetilde{D}_{\mathrm{res}}\Delta\Omega\right)}{\sin\left(\frac{\widetilde{D}_{\mathrm{res}}}{2}\Delta\Omega\right)}e^{j\widetilde{D}'_{\mathrm{pre}}\Delta\Omega} \quad (11)\end{aligned}$$

with

$$\widetilde{D}'_{\mathrm{pre}} = \widetilde{D}_{\mathrm{pre}} + \frac{N-1}{2}\widetilde{D}_{\mathrm{res}}. \quad (12)$$

For very small arguments of the sine functions, i.e., for

$$\frac{N}{2}|\widetilde{D}_{\mathrm{res}}\Delta\Omega| \ll 1 \quad (13)$$

(11) can finally be approximated as

$$\eta(\Delta\Omega) \approx N\eta_s(\Delta\Omega)e^{j\widetilde{D}'_{\mathrm{pre}}\Delta\Omega}. \quad (14)$$

Essentially, this is the N-fold transfer function of a single fiber with an additional phase shift governed by $\widetilde{D}'_{\mathrm{pre}}$. In this case, $\widetilde{D}'_{\mathrm{pre}}$ can be interpreted as the amount of dispersion precompensation of an equivalent single-span system, which becomes clear when comparing (14) to (8). Within the validity of the first-order perturbation approach and (13), systems with arbitrary single-periodic dispersion maps can thus be described by simple single-span systems. The performance of the single-span system and the N-span system will be comparable, provided that the average launch power P is scaled such that the overall average nonlinear phase shift [7]

$$\Phi_{\mathrm{NL}} = N\frac{\gamma P}{\alpha} \quad (15)$$

remains constant. However, the boundaries placed by (13) are quite strict. Should the approximation (14) be at least accurate for $\Delta\Omega \le \Omega_s$, it follows from (13) that $N|\widetilde{D}_{\mathrm{res}}| \ll 2|\beta_2|/\alpha$. This means that the cumulated residual dispersion over all spans has to be much less than the cumulated dispersion over twice the effective length of the transmission fiber. Extensive numerical simulations for OOK as well as differential phase-shift keying (DPSK) have shown that the match in terms of required OSNR penalty is reasonably good for $N|\widetilde{D}_{\mathrm{res}}| \le 0.8|\beta_2|/\alpha$, e.g., for five spans of SSMF, $D_{\mathrm{res}} \le 60\,\mathrm{ps/nm}$ [21], [22].

Fig. 3(a) shows the magnitude of the nonlinear transfer function for a system with large residual dispersion per span corresponding to 40 km uncompensated SSMF length. Clearly, the approximation of the main lobe, even for $\Delta\Omega < \Omega_s$ is very poor. On the other hand, the approximation is quite good for small residual dispersion per span as seen in Fig. 3(b).

C. Randomly Varying Residual Dispersion per Span

In practical transmission systems, residual dispersion per span (RDPS) usually varies from span to span due to a certain granularity of lumped dispersion-compensating modules (DCM), e.g., DCM-20 which compensate 20 km of SSMF are commonly used in 10 Gb/s systems. The model developed in the preceding section cannot be applied to these systems in

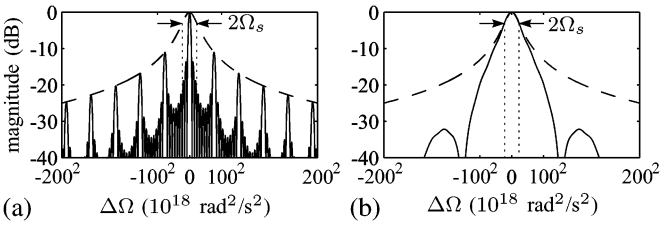

Fig. 3. Magnitude of the nonlinear transfer function for 10 × 80 km SSMF without dispersion precompensation and residual dispersion per span corresponding to (a) 40 km and (b) 2 km of SSMF. The dashed line shows the magnitude of $\eta_s(\Delta\Omega)$.

a straightforward manner. However, it is possible to find an approximate solution for the nonlinear transfer function of such systems provided that the RDPS does not differ too much from its mean value.

Let $\Delta\widetilde{D}_{\mathrm{res},i}$ be the deviation of the RDPS of the *i*th span from the mean RDPS $\langle\widetilde{D}_{\mathrm{res}}\rangle$, such that $\widetilde{D}_{\mathrm{res},i} = \langle\widetilde{D}_{\mathrm{res}}\rangle + \Delta\widetilde{D}_{\mathrm{res},i}$. The cumulated dispersion at the beginning of the *n*th span can then be expressed as

$$\widetilde{D}_n = \widetilde{D}_{\mathrm{pre}} + (n-1)\langle\widetilde{D}_{\mathrm{res}}\rangle + \sum_{i=0}^{n-1}\Delta\widetilde{D}_{\mathrm{res},i} \qquad (16)$$

where $\Delta\widetilde{D}_{\mathrm{res},0}$ accounts for a possible deviation of the precompensation from its nominal value. The RDPS mismatch $\Delta\widetilde{D}_{\mathrm{res},i}$ is uniformly distributed with mean zero and distribution boundaries defined by the employed DCM. Taking above example of DCM-20, the maximum mismatch corresponds to 10 km of SSMF (i.e., $-200\ \mathrm{ps}^2 \le \Delta\widetilde{D}_{\mathrm{res},i} \le 200\ \mathrm{ps}^2$).

Assuming small deviations $|\Delta\widetilde{D}_{\mathrm{res},i}| \ll |\beta_2/\alpha|$ for all spans and validity of (13) for $\widetilde{D}_{\mathrm{res}} = \langle\widetilde{D}_{\mathrm{res}}\rangle$, it can be shown that (9) may be approximated as

$$\eta(\Delta\Omega) \approx N\eta_s(\Delta\Omega)e^{j\frac{1}{N}\sum_{n=1}^{N}\widetilde{D}_n\Delta\Omega}. \qquad (17)$$

This leads to the same single-span representation as in (14) but with an equivalent precompensation of

$$\widetilde{D}'_{\mathrm{pre}} = \frac{1}{N}\sum_{n=1}^{N}\widetilde{D}_n. \qquad (18)$$

For the special case of periodic dispersion maps with nonrandom RDPS, the above equation reduces to the expression given in (12).

III. Numerical Results and Discussion

In order to apply the model to transmission of RZ-OOK signals, a single-span system is simulated numerically with the commercially available simulation tool VPItransmissionMaker which implements a split-step Fourier method.

A. System Setup

A general setup of a fiber-optic transmission system is shown in Fig. 4. The considered modulation format is RZ-OOK with

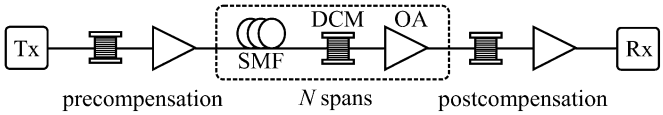

Fig. 4. Generic setup of a transmission line consisting of N spans.

a duty cycle of 33% in a single-channel and a five-channel WDM configuration, where the spectral efficiency of the WDM configuration is 0.4 bit/s/Hz. The transmitted data are de Bruijn binary sequences of length 2^{10}. Multiplexer and demultiplexer filters are modeled as second-order Gaussian bandpass filters with a 3-dB bandwidth of $2B$. A dispersion precompensation stage after the transmitter is followed by N spans, each consisting of a single-mode fiber (SMF), a dispersion compensation module (DCM), and an optical amplifier (OA). For all simulations, the SMF has an attenuation coefficient of $\alpha = 0.2\ \mathrm{dB/km}$ and a nonlinear coefficient of $\gamma = 1.31\ \mathrm{W^{-1}m^{-1}}$. All simulation results can be scaled to fibers with other attenuation and nonlinear coefficients by adjusting the launch power for constant nonlinear phase shift according to (15). Second-order group-velocity dispersion and the nonlinear impact of the DCM have not been considered. The optical amplifier compensates the span loss. The postcompensation stage in front of the receiver is adjusted such that the net residual dispersion is zero. The electrical filter after ideal square-law detection of the optical signal is a fifth-order Bessel low-pass filter with a cutoff frequency of $0.7B$. The bit-error ratio (BER) is estimated based on a Karhunen–Loève expansion (assuming additive white Gaussian noise before the optical demultiplexer filter) and saddle-point approximation [23].

B. Nonlinear Threshold of Systems With Single-Periodic Dispersion Map

In this section, the performance of RZ-OOK transmission is assessed by means of the nonlinear threshold as a criterion. The nonlinear threshold is defined as the average launch power that results in an OSNR penalty of 1 dB with respect to the required back-to-back OSNR for $\mathrm{BER} = 10^{-9}$. This is a very convenient measure since it is independent of the bit rate (i.e., the required back-to-back OSNR), and it ensures that the nonlinear perturbation δ_{NL} is small enough to verify the condition of a weakly nonlinear regime. Furthermore, it gives the maximum reasonable launch power into a system, since increasing the launch power beyond the nonlinear threshold would not yield a higher OSNR margin at the receiver due to additional nonlinear distortion of the signal.

Fig. 5 plots the nonlinear threshold for single-channel and WDM transmission versus the parameters B^2/Ω_s and $B^2\widetilde{D}'_{\mathrm{pre}}$ accounting for the type of the transmission fiber and cumulated dispersion profile, respectively. The lower bound of the abscissa corresponds to a bit rate of 10 Gb/s and a fiber dispersion of $D = 1\ \mathrm{ps/(nm{\cdot}km)}$, while the upper bound corresponds to $B = 160\ \mathrm{Gb/s}$ and $D = 18\ \mathrm{ps/(nm\cdot km)}$. Within the validity range of the model according to (13), this plot completely describes

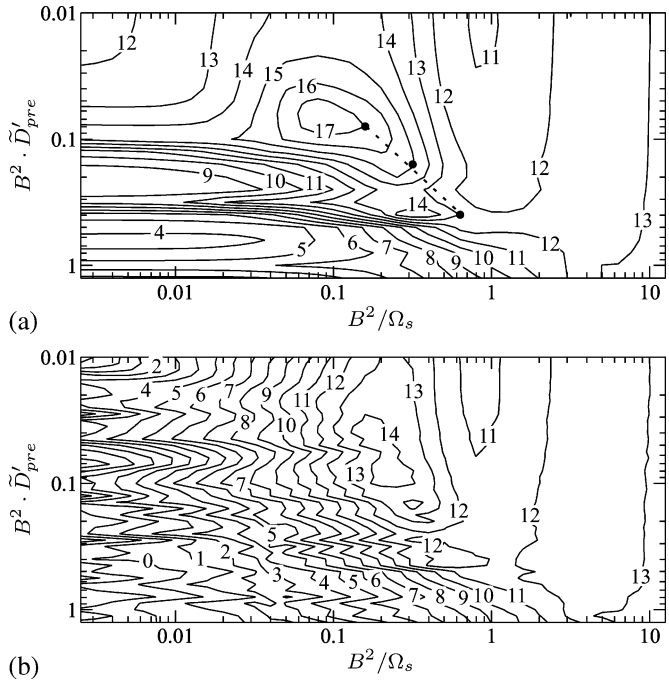

Fig. 5. Nonlinear threshold in dBm (contour line labels) for RZ-OOK modulation and transmission of (a) a single channel with the bit rate B or (b) a $5 \times B$ WDM signal over a single span with precompensation $\widetilde{D}'_{\mathrm{pre}}$. The dots indicate configurations giving maximum nonlinear threshold for $B = 40$ Gb/s and $D = 4, 8, 16$ ps/(nm · km).

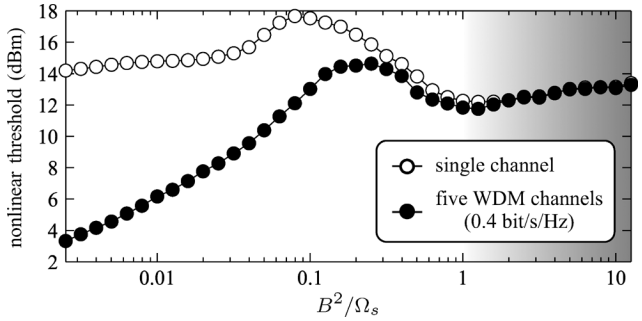

Fig. 6. Nonlinear threshold for optimized equivalent precompensation $\widetilde{D}'_{\mathrm{pre}}$ in the case of single channel (white circles) and $5 \times B$ WDM (black circles) transmission. Due to insufficient bit-sequence length, the nonlinear threshold is likely to be overestimated in the shaded area, i.e., for large channel memory.

the system performance for an arbitrary bit rate, fiber type and dispersion map.

For example, the points of maximum nonlinear threshold for a bit rate of 40 Gb/s and a fiber dispersion of $D = 4, 8, 16$ ps/(nm · km) are indicated by the dots in Fig. 5(a). With (12) the rule for optimum precompensation and residual dispersion per span derived in [10], [11] can be directly reproduced (dashed line in Fig. 5). Measurements of the nonlinear threshold e.g., in [24]–[26] of a simple single-span system can thus be used to estimate optimum dispersion map parameters and a lower bound for system reach of a certain modulation format.

The same approach can be used for WDM systems (Fig. 5(b)). However, the results are valid for a fixed number of WDM channels and fixed spectral efficiency only. Fig. 6 compares the maximum nonlinear threshold of single-channel transmission with that of WDM transmission at a spectral efficiency of 0.4 bit/s/Hz. It should be noted that the nonlinear threshold for $B^2/\Omega_s > 1$ (shaded region) is likely to be overestimated, since the length of the simulated binary sequence is not sufficient to correctly account for all intrachannel nonlinear distortions [16]. Indeed recent numerical results with sequence lengths up to 2^{17} indicate that the nonlinear threshold does not increase for larger values of B^2/Ω_s [27]. Further note should be taken that the results represent the nonlinear threshold due to nonlinear impairments in the absence of net residual dispersion. In certain scenarios the threshold can be further enhanced by careful optimization of the net residual dispersion, e.g., in SPM-limited systems (single-channel transmission at small B^2/Ω_s in Fig. 6) [28].

The comparison between single-channel and WDM transmission reveals the severe impact of FWM for small B^2/Ω_s, where the nonlinear threshold for WDM transmission can be up to 10 dB lower than for the single-channel case. In contrast, there is negligible penalty due to interchannel nonlinear effects for sufficiently large bit rate and/or dispersion ($B^2/\Omega_s \geq 0.3$), i.e., in the pseudolinear regime [20]. The maximum nonlinear threshold is achieved in a tradeoff between inter- and intrachannel nonlinear effects at $B^2/\Omega_s = 0.25$. Assuming available fiber with a maximum dispersion parameter of $D = 20$ ps/(nm·km), e.g., superlarge-effective-area fiber, the system reach could be maximized with a bit rate of about 20 Gb/s per channel as this would maximize the nonlinear threshold, while minimizing the required received OSNR under the given constraints. A similar analysis for binary and quaternary DPSK modulation can be found in [29].

C. Randomly Varying Residual Dispersion per Span

Due to length variations of the transmission fiber in each span and granularity of DCM, the nominal RDPS can usually not be guaranteed throughout a link. Therefore, it is important to estimate the consequences of an imperfect dispersion map on the transmission performance [30]. In this example, transmission of 5×40 Gb/s RZ-OOK over a link consisting of 10 spans is considered. The precompensation D_{pre} is varied from -700 ps/nm to 300 ps/nm in steps of 100 ps/nm. Two different uniform distributions of the RDPS are simulated:

1) mean RDPS: $\langle D_{\mathrm{res}} \rangle = \pm 40$ ps/nm, maximum deviation: $\Delta D_{\mathrm{res}} = \pm 40$ ps/nm (corresponding to a DCM-granularity of 5 km SSMF),
2) mean RDPS: $\langle D_{\mathrm{res}} \rangle = \pm 80$ ps/nm, maximum deviation $\Delta D_{\mathrm{res}} = \pm 80$ ps/nm (corresponding to a DCM-granularity of 10 km SSMF).

For negative precompensation values, a positive mean RDPS has been assumed and vice versa. This way all dispersion maps show either a monotonously increasing or decreasing cumulated dispersion at the beginning of each span. A special case occurs for zero precompensation, where the mean RDPS is assumed to be zero. The equivalent precompensation D'_{pre} is determined by (16) and (18). For each of the two distributions, 1100 random systems have been simulated. Fig. 7 plots the OSNR penalty with respect to the required back-to-back OSNR versus precompensation of the equivalent single-span system. Penalties

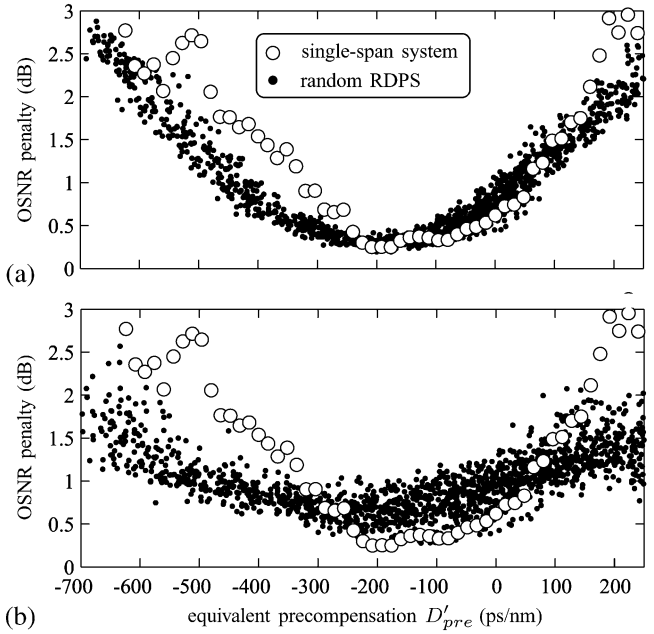

Fig. 7. OSNR penalty for different values of equivalent precompensation. Shown are the results of split-step Fourier simulations for transmission of 5 × 40 Gb/s RZ-OOK over different transmission lines: a single 80 km span with launch power of 12 dBm per channel (circles), and 10 × 80 km SSMF with uniformly distributed residual dispersion per span, varying precompensation and 2 dBm launch power per channel (dots). The distribution parameters are: (a) a mean of $\langle D_{\rm res}\rangle = \pm 40\ {\rm ps/nm}$ and a maximum deviation of $\Delta D_{\rm res} = \pm 40\ {\rm ps/nm}$ and (b) a mean of $\langle D_{\rm res}\rangle = \pm 80\ {\rm ps/nm}$ and a maximum deviation of $\Delta D_{\rm res} = \pm 80\ {\rm ps/nm}$.

for the equivalent single-span system (where $D'_{\rm pre} = D_{\rm pre}$) are shown as a reference (circles). As long as mean RDPS and RDPS variation are small enough, the qualitative match between the single-span system and random multispan systems is satisfactory (Fig. 7(a)). For equivalent precompensation in the range $-300\ {\rm ps/nm} \le D'_{\rm pre} \le 150\ {\rm ps/nm}$, the maximum error in OSNR penalty is less than ±0.5 dB. Also, the optimum system configuration around a precompensation of about −200 ps/nm is correctly estimated by the single-span system. However, for larger mean RDPS and larger variation per span (Fig. 7(b)) approximation by the single-span model becomes too inaccurate and the error in terms of OSNR penalty can approach 1 dB even near the predicted optimum. The results in Fig. 7(b) also indicate that the OSNR margin can be significantly reduced due to DCM granularity, even when special care is taken to match the optimum dispersion map as accurate as possible.

IV. Conclusion

The frequency-domain Volterra series expansion has been reviewed in the context of dispersion map evaluation. Starting from the Volterra transfer function of a concatenation of fiber sections, an approximate solution for single-periodic dispersion-managed systems with precompensation and randomly varying residual dispersion per span has been derived. In this context, it was shown that under certain conditions an arbitrary multispan system can be approximated by a simple equivalent single-span system, where the precompensation of the single-span system is defined through the dispersion map parameters of the multispan system. This simplified model was then applied to obtain optimum system parameters in the case of RZ-OOK modulation, arbitrary bit rate, and fiber type. The results indicate that without optimized net residual dispersion at the receiver, the system reach of WDM transmission with RZ-OOK modulation and a spectral efficiency of 0.4 bit/s/Hz can be maximized by using a bit rate of 20 Gb/s per channel and a superlarge-effective-area fiber with a dispersion parameter $D = 20\ {\rm ps/(nm\cdot km)}$. Furthermore, it was shown that the prediction of optimum system parameters by use of the single-span model even holds in the presence of small random variations of the residual dispersion per span. This is important since these variations inevitably occur in practical systems due to a given granularity of commercially available dispersion compensating modules.

Appendix I
The Nonlinear Transfer Function of a Single Fiber

Substituting (3) into (2), discarding all terms of higher order than 3 and comparing the terms of equal order yields two differential equations for the Volterra kernel transforms $H_1(\omega,z)$ and $H_3(\omega_1,\omega_2,\omega,z)$ [1]. They are solved by

$$H_1(\omega,z) = e^{\left(-\frac{\alpha}{2}+j\omega^2\frac{\beta_2}{2}\right)z} \tag{19}$$

and

$$H_3(\omega_1,\omega_2,\omega,z) = j\gamma H_1(\omega,z)\int_0^z e^{(-\alpha-j\beta_2\Delta\Omega)z'}dz' \tag{20}$$

where $\Delta\Omega = (\omega-\omega_1)(\omega_1-\omega_2)$. With (3), (19), and (20) the field envelope after propagation is

$$\tilde{A}(\omega,z) \approx H_1(\omega,z)\left(\tilde{A}_0(\omega)+\delta_{\rm NL}(\omega,z)\right) \tag{21}$$

where

$$\delta_{\rm NL}(\omega,z) = j\gamma\int\int\int_0^z e^{(-\alpha-j\beta_2\Delta\Omega)z'}dz'\tilde{S}_0 d\omega_1 d\omega_2 \tag{22}$$

is a small perturbation accounting for the impact of fiber nonlinearity on the signal [6]. Examination of (21) reveals a serious energy-divergence problem when the energy contained in the nonlinear perturbation gets too large. Therefore, (21) is valid in a weakly nonlinear regime only. This is covered in a greater detail in [5]. However, in the scope of this analysis, the nonlinear distortions are assumed small enough, such that the condition of a weakly nonlinear regime is fulfilled.

There are two distinct contributions to the nonlinear perturbation in (22), one stemming from the physical parameters of the fiber and the other from the input signal $\tilde{S}_0$. Thus, it makes sense to define a nonlinear transfer function to describe the signal-independent part of the nonlinear perturbation. With the nonlinear transfer function

$$\begin{aligned}\eta(\Delta\Omega,z) &= \gamma\int_0^z e^{(-\alpha-j\beta_2\Delta\Omega)z'}dz' \\ &= \frac{\gamma}{\alpha}\frac{1-e^{(-\alpha-j\beta_2\Delta\Omega)z}}{1+j\frac{\beta_2}{\alpha}\Delta\Omega}.\end{aligned} \tag{23}$$

The nonlinear perturbation can be concisely written as

$$\delta_{\mathrm{NL}}(\omega, z) = j \int\int \eta(\Delta\Omega, z)\tilde{S}_0 d\omega_1 d\omega_2. \tag{24}$$

For spatial coordinate $z \gg 1/\alpha$, the nonlinear transfer function $\eta(\Delta\Omega, z)$ can be approximated to be independent of z and reduces to $\eta_s(\Delta\Omega)$ as in (7).

Appendix II
The Nonlinear Transfer Function of Multiple Fiber Sections

Practical fiber-optic transmission systems consist of several concatenated fiber sections. The physical parameters of the fibers, such as length, group-velocity dispersion, attenuation and nonlinear coefficient are likely to be different in each section. Furthermore, the signal has to be amplified in certain intervals. This can either be done between fiber sections with discrete amplifiers such as e.g., erbium-doped fiber amplifiers (EDFA) or distributed along the fiber using a Raman amplification scheme [31]. Peddanarappagari and Brandt-Pearce derived a solution for the field envelope after transmission over several fiber sections including lumped amplifiers and amplifier noise in [32]. However, due to its complexity it is quite unwieldy and does not lend itself easily to analytic examination. In the following derivation amplifier noise and consequently any nonlinear interaction between the signal and amplifier noise are not considered.

To derive the nonlinear transfer function of a system consisting of multiple-fiber sections and amplifiers, including different amplification and dispersion compensation schemes, it is useful to define gain and dispersion profiles of the transmission link [6]. The gain profile can be defined as

$$\frac{\mathrm{d}G(z)}{\mathrm{d}z} = -\alpha(z) + g(z) + \sum_i g_i \delta(z - z_i) \tag{25}$$

where $G(z)$ is the accumulated gain, $g(z)$ accounts for distributed amplification, g_i is the gain of lumped amplifiers positioned at z_i and $\delta(z)$ is Dirac's delta function. Similarly, the dispersion profile can be defined as

$$\frac{\mathrm{d}\widetilde{D}(z)}{\mathrm{d}z} = -\beta_2(z) - \sum_j \widetilde{D}_j \delta(z - z_j) \tag{26}$$

where $\widetilde{D}(z)$ is the overall cumulated dispersion at position z and $\widetilde{D}_j$ is the cumulated dispersion of a lumped dispersion compensation module at position z_j.

The field envelope at the output of the mth fiber section can be expressed with the recursion

$$\tilde{A}_m(\omega) \approx H_{1,m}(\omega, L_m) \times \left(\tilde{A}_{m-1}(\omega) + j \int\int \eta_m(\Delta\Omega, L_m)\tilde{S}_{m-1} d\omega_1 d\omega_2 \right) \tag{27}$$

where $\tilde{S}_i = \tilde{A}_i(\omega_1)\tilde{A}_i^*(\omega_2)\tilde{A}_i(\omega_3)$ and $H_{1,m}$, η_m, and L_m are the first-order kernel transform, the nonlinear transfer function and the length of the mth fiber section, respectively. Please note that since the nonlinear perturbation generated in each span is assumed to be very small, it is neglected when calculating $\tilde{S}_{m-1}$. With (27) the output field envelope $\tilde{A}_{\mathrm{M}}(\omega)$ after transmission over M fiber sections is

$$\tilde{A}_{\mathrm{M}}(\omega) \approx \prod_{m=1}^{\mathrm{M}} H_{1,m}(\omega, L_m) \left(\tilde{A}_0(\omega) + \sum_{m=1}^{\mathrm{M}} \delta_{NL,m}(\omega) \right) \tag{28}$$

where

$$\delta_{NL,m}(\omega) = j\gamma_m \int\int \int_{z_{m-1}}^{z_m} e^{G(z) + j\widetilde{D}(z)\Delta\Omega} dz \tilde{S}_0 d\omega_1 d\omega_2 \tag{29}$$

is the nonlinear perturbation generated in the mth fiber section with $z_0 = 0$, $L_m = z_m - z_{m-1}$, and γ_m the length and nonlinear coefficient of the mth fiber and gain and dispersion profiles $G(z)$ and $\widetilde{D}(z)$ as defined in (25) and (26). To get a similar notation as in the single-fiber case, the overall nonlinear perturbation can be noted as

$$\begin{aligned} \delta_{\mathrm{NL}}(\omega) &= \sum_{m=1}^{\mathrm{M}} \delta_{NL,m}(\omega) \\ &= j \int\int \eta(\Delta\Omega)\tilde{S}_0 d\omega_1 d\omega_2 \end{aligned} \tag{30}$$

with the overall nonlinear transfer function of a concatenation of M fiber sections

$$\eta(\Delta\Omega) = \sum_{m=1}^{\mathrm{M}} \gamma_m \int_{z_{m-1}}^{z_m} e^{G(z) + j\widetilde{D}(z)\Delta\Omega} dz. \tag{31}$$

It is easily verified that (23) is a special case of the above equation with $M = 1$, no dispersion precompensation and no distributed amplification. Further simplification is possible by noting that the product of first-order kernel transforms in (28) essentially describes the residual gain $G(z_{\mathrm{M}})$ and dispersion $\widetilde{D}(z_{\mathrm{M}})$ at the receiver. The overall first-order kernel transform of the transmission line can thus be defined as

$$H_1(\omega) = \prod_{m=1}^{\mathrm{M}} H_{1,m}(\omega, L_m) = e^{G(z_{\mathrm{M}}) + j\widetilde{D}(z_{\mathrm{M}})\Delta\Omega}. \tag{32}$$

Analogous to the solution for a single fiber in (21) and (28) can now be written as

$$\tilde{A}_{\mathrm{M}}(\omega) \approx H_1(\omega) \left(\tilde{A}_0(\omega) + \delta_{\mathrm{NL}}(\omega) \right). \tag{33}$$

References

[1] K. V. Peddanarappagari and M. Brandt-Pearce, "Volterra series transfer function of single-mode fibers," *J. Lightw. Technol.*, vol. 15, no. 12, pp. 2232–2241, Dec. 1997.

[2] B. Xu and M. Brandt-Pearce, "Comparison of FWM- and XPM-induced crosstalk using the Volterra series transfer function method," *J. Lightw. Technol.*, vol. 21, no. 1, pp. 40–53, Jan. 2003.

[3] X. Wei, "Power-weighted dispersion distribution function for characterizing nonlinear properties of long-haul optical transmission links," *Opt. Lett.*, vol. 31, no. 17, pp. 2544–2546, Sep. 2006.

[4] A. Vannucci, P. Serena, and A. Bononi, "The RP method: A new tool for the iterative solution of the nonlinear Schrödinger equation," *J. Lightw. Technol.*, vol. 20, no. 7, pp. 1102–1112, Jul. 2002.

[5] B. Xu and M. Brandt-Pearce, "Modified Volterra series transfer function method," *IEEE Photon. Technol. Lett.*, vol. 14, no. 1, pp. 47–49, Jan. 2002.
[6] H. Louchet, A. Hodžić, K. Petermann, A. Robinson, and R. Epworth, "Simple criterion for the characterization of nonlinear impairments in dispersion-managed optical transmission systems," *IEEE Photon. Technol. Lett.*, vol. 17, no. 10, pp. 2089–2091, Oct. 2005.
[7] J.-C. Antona, S. Bigo, and J.-P. Faure, "Nonlinear cumulated phase as a criterion to assess performance of terrestrial WDM systems," in *Proc. OFC 2002*, Anaheim, CA, paper WX5.
[8] B. Konrad and K. Petermann, "Optimum fiber dispersion in high-speed TDM systems," *IEEE Photon. Technol. Lett.*, vol. 13, no. 4, pp. 299–301, Apr. 2001.
[9] A. Cauvin, Y. Frignac, and S. Bigo, "Nonlinear impairments at various bit rates in single-channel dispersion-managed systems," *Electron. Lett.*, vol. 39, no. 23, pp. 1670–1671, Nov. 2003.
[10] R. I. Killey, H. J. Thiele, V. Mikhailov, and P. Bayvel, "Reduction of intrachannel nonlinear distortion in 40-Gb/s-based WDM transmission over standard fiber," *IEEE Photon. Technol. Lett.*, vol. 12, no. 12, pp. 1624–1626, Dec. 2000.
[11] Y. Frignac, J.-C. Antona, and S. Bigo, "Enhanced analytical engineering rule for fast optimization of dispersion maps in 40 Gbit/s-based transmission," in *Proc. OFC 2004*, Los Angeles, CA, paper TuN3.
[12] G. P. Agrawal, *Nonlinear Fiber Optics*, 4th ed. CA: Academic Press, Dec. 2006.
[13] J. P. Gordon and L. F. Mollenauer, "Phase noise in photonic communications systems using linear amplifiers," *Opt. Lett.*, vol. 15, no. 23, pp. 1351–1353, Dec. 1990.
[14] S. K. Turitsyn, E. G. Turitsyna, S. B. Medvedev, and M. P. Fedoruk, "Averaged model and integrable limits in nonlinear double-periodic Hamiltonian systems," *Physical Review E*, vol. 61, no. 3, pp. 3127–3132, Mar. 2000.
[15] S. K. Turitsyn, M. P. Fedoruk, E. G. Shapiro, V. K. Mezenrsev, and E. G. Turitsyna, "Novel approaches to numerical modeling of periodic dispersion-managed fiber communication systems," *IEEE J. Sel. Topics Quantum Electron.*, vol. 6, no. 2, pp. 263–275, Mar./Apr. 2000.
[16] L. K. Wickham, R.-J. Essiambre, A. H. Gnauck, P. J. Winzer, and A. R. Chraplyvy, "Bit pattern length dependence of intrachannel nonlinearities in pseudolinear transmission," *IEEE Photon. Technol. Lett.*, vol. 16, no. 6, pp. 1591–1593, Jun. 2004.
[17] P. Bayvel and R. I. Killey, "Nonlinear optical effects in WDM transmission," in *Optical Fiber Telecommunications IVB*. CA: Academic Press, 2002, pp. 611–641.
[18] P. J. Winzer and R.-J. Essiambre, "Advanced optical modulation formats," *Proc. IEEE*, vol. 9, no. 5, pp. 952–985, May 2006.
[19] C. Peucheret, N. Hanik, R. Freund, L. Molle, and P. Jeppesen, "Optimization of pre- and post-dispersion compensation schemes for 10-Gbits/s NRZ links using standard and dispersion compensating fibers," *IEEE Photon. Technol. Lett.*, vol. 12, no. 8, pp. 992–994, Aug. 2000.
[20] R.-J. Essiambre, G. Raybon, and B. Mikkelsen, "Pseudo-linear transmission of high-speed TDM signals: 40 and 160 Gb/s," in *Optical Fiber Telecommunications IVB*. NJ: Academic Press, 2002, pp. 232–304.
[21] J. K. Fischer, C.-A. Bunge, K. Jamshidi, H. Louchet, and K. Petermann, "Equivalent dispersion maps in fiber-optic communication system," in *Proc. ECOC 2006*, Cannes, France, paper We3.P.134.
[22] J. K. Fischer, C.-A. Bunge, and K. Petermann, "Application of the nonlinear transfer function to dispersion map evaluation in DPSK transmission systems," in *Proc. LEOS 2006*, Montreal, Canada, paper ThH2.
[23] E. Forestieri, "Evaluating the error probability in lightwave systems with chromatic dispersion, arbitrary pulse shape and pre- and postdetection filtering," *J. Lightw. Technol.*, vol. 18, no. 11, pp. 1493–1503, Nov. 2000.
[24] R. Dischler, A. Klekamp, J. Lazaro, and W. Idler, "Experimental comparison of non linear threshold and optimum pre dispersion of 43 Gb/s ASK and DPSK formats," in *Proc. OFC 2004*, Los Angeles, CA, paper TuF4.
[25] A. Klekamp, R. Dischler, and W. Idler, "Fiber nonlinear threshold comparison of SMF and NZDSF types on binary 43 Gb/s modulation formats," in *Proc. ECOC 2005*, Glasgow, Scotland, paper We4.P.059.
[26] A. Klekamp, R. Dischler, and W. Idler, "DWDM and single channel fiber nonlinear thresholds for 43 Gb/s ASK and DPSK formats over various fiber types," in *Proc. OFC 2006*, Anaheim, CA, paper OFD5.
[27] P. Serena, A. Orlandini, and A. Bononi, "The memory of optimized dispersion-managed periodic optical links," in *Proc. ECOC 2007*, Berlin, Germany, paper PO93.
[28] G. Bellotti, A. Bertaina, and S. Bigo, "Dependence of self-phase modulation impairments on residual dispersion in 10-Gb/s-based terrestrial transmissions using standard fiber," *IEEE Photon. Technol. Lett.*, vol. 11, no. 7, pp. 824–826, Jul. 1999.
[29] J. K. Fischer and K. Petermann, "Nonlinear threshold of RZ-DBPSK and RZ-DQPSK," in *Proc. ECOC 2008*, Brussels, Belgium, paper P.4.19.
[30] C. Xie, L. F. Mollenauer, and N. Mamysheva, "Numerical study of random variations of span lengths and span path-average dispersions on dispersion-managed soliton system performance," *J. Lightw. Technol.*, vol. 21, no. 3, pp. 769–775, Mar. 2003.
[31] G. P. Agrawal, "Optical amplifiers," in *Fiber-Optic Communication Systems*, 3rd ed. NJ: Wiley & Sons, 2002, ch. 6, pp. 226–278.
[32] K. V. Peddanarappagari and M. Brandt-Pearce, "Volterra series approach for optimizing fiber-optic communications system designs," *J. Lightw. Technol.*, vol. 16, no. 11, pp. 2046–2055, Nov. 1998.

Johannes Karl Fischer (S'04) was born in Berlin, Germany in 1976. He studied electrical engineering at the Technische Universität Berlin, Germany and the University of Manchester, UK. In 2003, he received the Dipl.-Ing. degree in electrical engineering from the Technische Universität, Berlin. In 2005, he received a best student paper award of the Asia-Pacific Optical Communications Conference.

He is currently pursuing his Ph.D. degree at the Technische Universität Berlin. His research interests are advanced modulation formats and fiber nonlinearity.

Christian-Alexander Bunge (S'01–M'03) received a diploma in electrical engineering in 1999 and a Ph.D. from the Technische Universität Berlin in 2003. He studied the propagation and attenuation properties of plastic optical fibers and of multimode fibers. 2002–2004 he was with the POF-AC of the University of Applied Sciences in Nuremberg, Germany, as a research fellow and responsible for international projects. Since 2004, he is with the Technische Universität Berlin as a senior scientist. His current scientific work deals with modelling of multimode fibers, equalization and optical signal processing.

Klaus Petermann (F'09) was born in Mannheim, Germany in 1951. He received the Dipl.-Ing. degree in 1974 and the Dr.-Ing. degree in 1976, both in electrical engineering from the Technische Universität Braunschweig, Germany. From 1977 to 1983 he was with AEG-Telefunken, Ulm, Germany, where he was engaged in research work on semiconductor lasers, optical fibers, and optical fiber sensors. In 1983, he became a full professor at the Technische Universität Berlin, where his research interests are concerned with optical fiber communications and integrated optics. In 1993, Dr. Petermann was awarded with the Leibniz-award from the Deutsche Forschungsgemeinschaft (German research council). In 1999/2000, he received the "distinguished lecturer"-award from the IEEE Lasers and Electro-Optics Society.

From 1999–2004, he was an associate editor for IEEE PHOTONICS TECHNOLOGY LETTERS and from 1996–2004 he was a member of the board of the VDE. From 2004–2006, he was Vice President for research at the Technische Universität Berlin and from 2001–2008 he was member of the Senate of the Deutsche Forschungsgemeinschaft. Dr. Petermann is a senior member of the IEEE and a member of the Berlin-Brandenburg academy of science.